

Journal of
**Applied
Crystallography**
ISSN 0021-8898
Editor: **Gernot Kosterz**

Absorption corrections for diamond-anvil pressure cells implemented in the software package *Absorb6.0*

R. J. Angel

Copyright © International Union of Crystallography

Author(s) of this paper may load this reprint on their own web site provided that this cover page is retained. Republication of this article or its storage in electronic databases or the like is not permitted without prior permission in writing from the IUCr.

Absorption corrections for diamond-anvil pressure cells implemented in the software package *Absorb6.0*

R. J. Angel

Crystallography Laboratory, Department of GeoSciences, Virginia Tech, Blacksburg, VA 24060, USA.
Correspondence e-mail: rangel@vt.eduReceived 15 December 2003
Accepted 5 March 2004© 2004 International Union of Crystallography
Printed in Great Britain – all rights reserved

High-pressure single-crystal structure refinement requires intensity data that have been corrected for the various absorption effects in the pressure cell. In this contribution, the methods for calculating the absorption corrections for a transmission-geometry diamond-anvil pressure cell are reviewed. The ideas presented in this paper have been implemented in a software package for Microsoft Windows, *Absorb6.0*, available at <http://www.crystal.vt.edu/>.

1. Introduction

As high-pressure studies of crystal structures become more widespread, there is a corresponding need for additional software tools to handle the data reduction issues that arise in addition to processing diffraction data collected from crystals in air. The most commonly used type of high-pressure device is the transmission-geometry diamond-anvil cell (DAC), which in its various guises (e.g. Miletich *et al.*, 2000) is suitable for both single-crystal and powder X-ray diffraction on both laboratory diffractometers and synchrotron sources.

There are many types of transmission diamond-anvil pressure cells (see Miletich *et al.*, 2000), but their essential features from the point of view of absorption corrections are illustrated in Fig. 1. The incident and diffracted X-ray beams pass through the DAC at low angles of inclination to the load axis. For single-crystal studies, the crystal is mounted on the culet face of one of the two diamond anvils. An enclosed sample chamber is formed by the faces of the two opposed anvils and a metal foil drilled with a 'gasket hole' of a diameter less than that of the culet faces of the anvils. The gasket hole is filled with a pressure medium, usually a fluid or a gas. The X-ray beams passing through the cell are therefore partially absorbed by the backing plates, the anvils, the pressure fluid and the crystal, as well as partially by the gasket when the beams pass at high angles to the load axis of the cell. As a result, intensity data collected from crystals in such a DAC show a strong variation with the angle of inclination of the beams to the load axis, as demonstrated by the Ψ -scan data in Fig. 2. It is this variation due to absorption that needs to be corrected if the data are to be used to produce accurate refinements of the crystal structure. In addition, there are sharp dips in the intensities of the reflection at specific setting angles (Fig. 2) that are attributable to simultaneous diffraction events in the diamond anvils (Loveday *et al.*, 1990). As diffraction events, these cannot be corrected by an absorption program, but are identified and rejected during the averaging of the data set.

In §2 of this contribution, the general issues involved in making the absorption corrections for intensity data collected from single crystals held at high pressures in transmission diamond-anvil pressure cells are laid out and a general expression for the transmission function is derived. This is followed in §3 by a description of how the necessary calculations have been implemented in a program, *Absorb6.0*, which is a development of the *Absorb* program originally written by

Burnham (1966), but not related to other programs of the same name (e.g. DeTitta, 1985).

2. General considerations

The transmission factor, T , often called the 'transmission coefficient', corrects the measured diffracted beam intensities for absorption as $I_{\text{corr}} = I_{\text{obs}}T^{-1}$. The transmission factor is different for different reflections from the same crystal because the path lengths of the incident and diffracted beams within the crystal are different. For a crystal mounted in air, the transmission factor for each reflection is given by the integral over the crystal volume, V , of the path lengths of the incident (t_i) and diffracted beams (t_D):

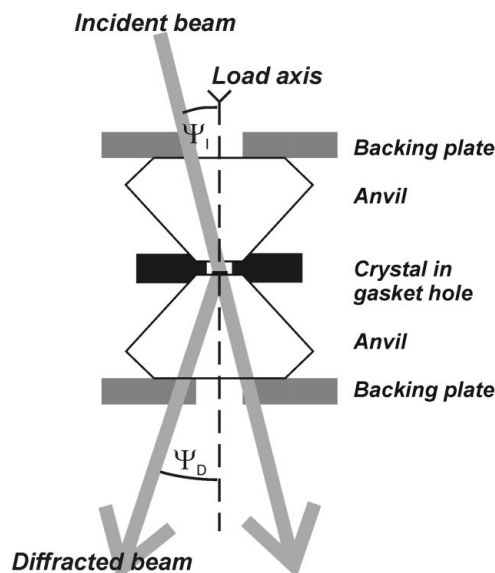
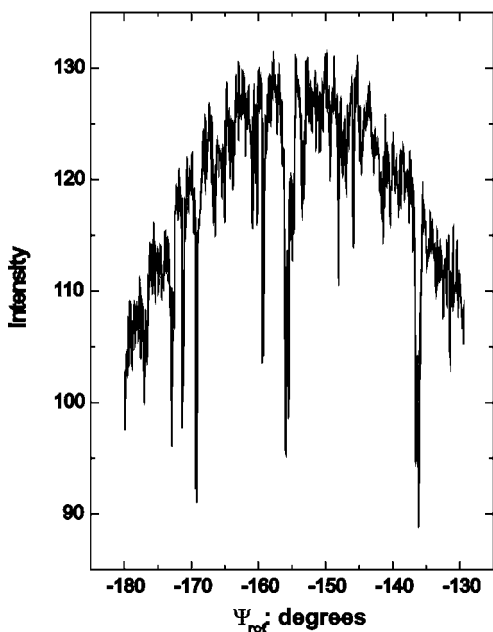


Figure 1

The essential features of a transmission-geometry diamond-anvil cell shown in cross section. The incident beam enters the cell through one backing plate and anvil at an angle Ψ_I to the load axis of the cell. The diffracted beam from the crystal leaves the cell through the other anvil and backing plate at an angle Ψ_D to the load axis. For the purposes of absorption, the cell is cylindrically symmetric about the load axis.


Figure 2

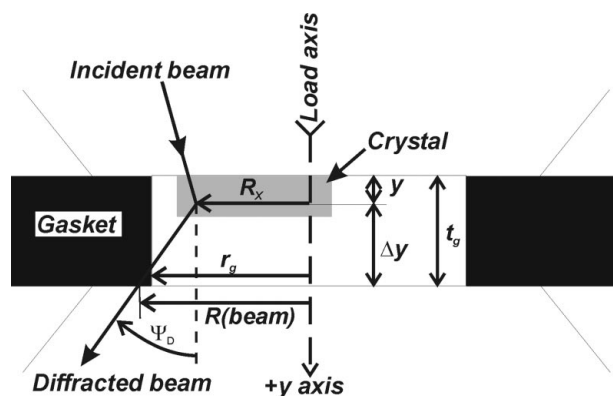
The variation of intensity with Ψ rotation of the $2\bar{2}0$ reflection at 0.1° intervals in Ψ_{rot} from a crystal of YAlO_3 ($\mu_1 = 320 \text{ cm}^{-1}$) held at 7.11 GPa in an ETH design (Miletich *et al.*, 2000) of diamond-anvil cell. Data were collected on an Xcalibur-1 instrument equipped with a point detector. The general fall-off in intensity with increasing inclination angle is due to absorption by the components of the pressure cell and the crystal. The sharp dips in intensity are due to simultaneous diffraction events in the diamond anvils (Loveday *et al.*, 1990) and cannot be corrected by absorption calculations.

$$T = V^{-1} \int_V \exp[-\mu(t_i + t_D)] dV. \quad (1)$$

When the incident and diffracted beams pass through other materials in addition to the crystal, such as a glass capillary, a furnace wall or a pressure cell, the general expression for the transmission coefficient of the beam becomes (*e.g.* Santoro *et al.*, 1968):

$$T = V^{-1} \int_V \exp\left[-\sum_i \mu_i(t_{i_i} + t_{D_i})\right] dV. \quad (2)$$

The factor $\exp[-\sum_i \mu_i(t_{i_i} + t_{D_i})]$ is the total transmission factor associated with a volume element dV of the crystal. In the summation, the μ_i are the linear absorption coefficients and the t_{i_i} and t_{D_i} are


Figure 3

The geometry of shadowing of the crystal by the gasket in the DAC illustrated for the case of the diffracted beam from one point in the crystal at a distance R_x from the load axis and depth y in the cell. In this case $\Delta y = t_g - y$, and $R(\text{beam}) = (\Delta y \tan \Psi_D + R_x) > r_g$. The path length of the diffracted beam in the gasket is thus $[R(\text{beam}) - r_g]/\sin \Psi_D$.

the path lengths for the incident and diffracted X-ray beams in each different material i , including the sample crystal itself. Note that even with the presence of other materials in the beam paths, the integral for the transmission factor is performed only over the crystal volume.

For transmission pressure cells the incident and diffracted X-ray beams pass through the DAC at low angles of inclination to the load axis (Fig. 1). These angles of inclination are traditionally denoted as Ψ_I for the incident beam and Ψ_D for the diffracted beam (Hazen, 1976). This contrasts with ‘transverse geometry’ cells in which one or both of the incident and diffracted beams are almost perpendicular to the load axis with $\Psi_I \simeq \Psi_D \simeq 90^\circ$. Note that these angles Ψ_I and Ψ_D are not the same as rotations about the diffraction vector that are traditionally denoted as ‘ Ψ scans’ (Busing & Levy, 1967), which will be distinguished in this paper as Ψ_{rot} .

The backing plates and the anvils in transmission cells are designed to be cylindrically symmetric about the load axis. The absorption correction for each of these components therefore only varies as a function of the Ψ_I or Ψ_D angle of the X-ray beam. Furthermore, to a good approximation, the correction for absorption by these cell components is the same for every point in the crystal for a given angle of inclination. The term $\exp(-\mu t)$ for each of these cell components can therefore be removed as a constant of multiplication from inside the integral in equation (2) and applied as a multiplier to the separately calculated absorption correction due to the crystal and other materials (Santoro *et al.*, 1968). Thus

$$T = V^{-1} T(\Psi_I) T(\Psi_D) \int_V \exp\left[-\sum_i \mu_i(t_{i_i} + t_{D_i})\right] dV, \quad (3)$$

in which $T(\Psi)$ denotes the transmission function for an incident or diffracted beam in a single backing plate and anvil. Note that, in the absence of gasket shadowing or absorption by the pressure medium, the transmission factor for the crystal could therefore be calculated by a conventional absorption program and the corrections for the diamond-cell absorption applied separately.

The pressure media used in diamond-cell experiments are usually frozen liquids such as alcohols or frozen gases such as hydrogen, helium or nitrogen. The absorption coefficients of such materials are so low that they can be generally ignored, but for other pressure media it may be necessary to calculate the contribution of the media to the transmission function. At higher Ψ angles there is also the possibility that part of either the incident or the diffracted beam will intersect the gasket, an effect which has become known as ‘gasket shadowing’. Because the path lengths of the beam through the pressure medium and the gasket will differ from point to point within the crystal, these contributions cannot be removed from the integrals in equations (2) and (3). On expansion of the summation in equation (3) to include these contributions, the overall expression for the transmission function of the DAC becomes

$$T = V^{-1} T(\Psi_I) T(\Psi_D) \int_V \exp[-\mu_x(t_{1,x} + t_{D,x})] \times \exp[-\mu_g(t_{1,g} + t_{D,g})] \exp[-\mu_m(t_{1,m} + t_{D,m})] dV. \quad (4)$$

In this expression, the various t_i and t_D are the path lengths of the incident and diffracted beams in the various materials comprising the loaded DAC, with the subscripts x , g and m denoting the crystal, gasket and pressure medium respectively.

Note that in transmission-geometry DACs, only the incident or the diffracted beam will be affected by gasket shadowing for reasonably thin crystals because the other beam will pass directly from the crystal into the underlying diamond anvil (*e.g.* Fig. 1). Furthermore, the shadowing only becomes significant if the crystal occupies a significant portion of the cross-sectional area of the gasket hole, or if it is

significantly displaced from the center of the hole. For example, no gasket shadowing occurs for a centered crystal of radius R_x in a gasket hole of radius r_g and thickness t_g provided that $\tan \Psi \leq (r_g - R_x)/t_g$ (Fig. 3). For most transmission DACs, the Ψ_I and Ψ_D angles are limited to $<45^\circ$ by the body of the cell. Shadowing therefore only becomes significant if the space between the crystal and the edge of the gasket becomes less than the thickness of the gasket between the anvils (perhaps 50–60 μm at 10 GPa for steel gaskets).

3. Implementation

3.1. Conventions and orientation

In order for the program to calculate the correct path lengths for the incident and diffracted X-ray beams in both the crystal and the DAC (if present), the reflection data, the crystal shape, and the DAC must all be described on a self-consistent set of coordinate axes, diffractometer circle parities and zero positions. Internally the *Absorb* program uses the axial conventions and circle parities defined by Busing & Levy (1967). These conventions also define the ‘normal-beam equatorial geometry’ of Arndt & Willis (1966), subsequently generalized by Dera & Katrusiak (1998). Because the DAC is rigidly fixed to the φ axis of the goniometer system *via* the goniometer head, the Cartesian ‘ φ axis’ coordinate system of Busing & Levy (1967) is the natural and easiest choice for making absorption corrections for the DAC. We additionally define the origin of the coordinate system to lie at the middle of the culet face of the anvil on the incident-beam side of the DAC. This point is assumed to be coincident with the center of the goniometer.

If the DAC is aligned, as is normally the case, with the load axis of the cell parallel to the incident beam direction when all of the diffractometer angles are zero and is fixed rigidly to the φ axis of the diffractometer during a measurement, then the load axis of the cell remains parallel to the y axis of the φ -axis coordinate system of Busing & Levy (1967). Therefore the angles Ψ_I and Ψ_D are given by the direction cosines of the incident and diffracted beams with respect to the y axis of the φ -axis system.

Absorb has been developed to handle both *SHELX* HKLF4 data files and the *int* format data files used by *RFINE* and related programs (Finger & Prince, 1974), and could be extended to read other file formats if required. The *RFINE* format was designed for point detector data and includes the goniometer setting angles with each reflection from which the Ψ_I and Ψ_D angles can be obtained directly as (Busing & Levy, 1967)

$$\begin{aligned} \cos(\Psi_I) &= \sin(\theta + \omega) \cos \chi \sin \varphi - \cos(\theta + \omega) \cos \varphi, \\ \cos(\Psi_D) &= \sin(\theta - \omega) \cos \chi \sin \varphi + \cos(\theta - \omega) \cos \varphi. \end{aligned} \quad (5)$$

In order to make the *Absorb* program usable in conjunction with any diffractometer, the circle parities and the axial orientation of the φ -axis system used to define the orientation matrix can be specified by the user.

For diffractometers equipped with area detectors, the value of Ψ_I is the same as in equation (5) because it only depends on the orientation of the DAC with respect to the incident beam. The value of Ψ_D depends on both the setting angles and the position at which the diffracted beam intersects the detector, which could be determined during integration of the raw data images. In practice, the integration software supplied for most diffractometers equipped with area detectors actually provides the beam path information of both the incident and the diffracted beam as the direction cosines with respect to the crystal axes, along with the integrated intensities in data files with the *SHELX* HKLF4 format. Within the *Absorb* code, the method

of Allan *et al.* (2000) is used to convert these direction cosines to the Busing–Levy φ -axis system and hence provide Ψ_I and Ψ_D directly from the direction cosines with respect to the y axis of that axis system. For some applications, such as measurement of diffuse scattering, area-detector data have to be corrected directly, pixel by pixel. While this would be possible with *Absorb*, the method described by Scheidegger *et al.* (2000) would be more efficient. However, if gasket shadowing corrections have to be performed, the method of Scheidegger *et al.* (2000) is not valid because then the transmission function T [equation (4)] no longer varies slowly as a function of position on each data image.

3.2. Anvils and backing plates

The anvils and backing plates contribute together to the transmission function $T(\Psi)$ which is calculated separately from the absorption due to the crystal. There are several different types of backing plates for transmission cells and these influence the choice of method to describe $T(\Psi)$ to the program. If the optical access hole in a beryllium backing plates is filled with a Be plug during data collections (*e.g.* Allan *et al.*, 1996), the absorption of each beam by one half of the pressure cell simply becomes that of two infinite flat plates, one made of diamond and one of Be, and the transmission factor becomes

$$T(\Psi) = \exp[-(\mu_{\text{Dia}} T_{\text{Dia}} + \mu_{\text{P}} T_{\text{P}}) / \cos \psi], \quad (6)$$

in which the T_{Dia} and T_{P} are the thicknesses of the anvil and platen (not the path lengths), respectively. If X-ray opaque seats are used to support the diamond anvils, then only correction for absorption by the anvil is necessary. In these cases $T(\Psi)$ can clearly be specified by the thickness and absorption coefficients of the components of the pressure cell.

An equivalent method that is more amenable to direct experimental measurement is to express the absorption curve for each side of the cell in terms of a single parameter $\xi = (\mu_{\text{Dia}} T_{\text{Dia}} + \mu_{\text{P}} T_{\text{P}})$. The relative absorption of a beam inclined at an angle Ψ to the cell axis is given by

$$I(\Psi)/I(\Psi = 0) = \exp[\xi(1 - 1/\cos \Psi)]. \quad (7)$$

In this case, the single parameter ξ can be determined by measuring the transmission of a very finely collimated direct beam through one-half of the cell without a gasket as a function of the cell rotation Ψ . Sufficiently fine collimation can be obtained through use of the needle from a hypodermic syringe (*e.g.* Wittlinger *et al.*, 1997; Boldyreva *et al.*, 1998) or a purpose-built collimator; 100 μm diameter is suitable. These direct measurements of DAC absorption must be made with a monochromated incident beam, otherwise the transmission of the *Bremstrahlung* component of the incident beam reduces the apparent absorption coefficient. These measurements should not be performed with a gasket and a regular collimator (*e.g.* Hazen, 1976), because then the measured transmitted intensity is that of a direct beam whose diameter is that of the gasket hole, and it also includes the cut-off of the beam by the decreasing apparent area of the gasket hole itself as the Ψ angle is increased (Finger & King, 1978; Malinowski, 1987; Ahsbahs, 1987). It therefore becomes a combined absorption plus shadowing correction, which may not be appropriate for intensities from a crystal smaller than the gasket hole (Finger & King, 1978).

In the original design of the Merrill–Bassett DAC and its derivatives (see Miletich *et al.*, 2000, for a review), the Be backing plates were drilled with cylindrical optical access holes that were left unfilled for data collection. At high inclination angles, when the beam does not pass through the access hole, the absorption correction reduces to

that given in equation (6). But at smaller values of Ψ , the beam passes partly or completely through the hole, producing a sharp step in the absorption as a function of Ψ (e.g. Hazen, 1976; Angel *et al.*, 2000). In other cells the backing plates are not flat plates. The absorption curves for any of these cases are best measured experimentally by transmission of the direct beam as described above and supplied to the program as a series of points of $T(\Psi)$ against Ψ .

A very different experimental approach to determining DAC absorption and shadowing is to calculate correction factors based upon a comparison of intensities collected from a crystal in the DAC without pressure fluid with those collected from the same crystal mounted in air (e.g. D'Amour *et al.*, 1978). In principle, this provides a correction term for both the absorption by the cell and the appropriate shadowing by the gasket, but the latter in particular will change at higher pressures as the gasket is thinned and is therefore neither recommended nor implemented within the *Absorb* program.

3.3. Crystal, gasket shadowing and pressure medium

The absorption by a crystal alone can be calculated by a number of methods that employ direct integration over the crystal volume by dividing it into Howells polyhedra (e.g. de Meulenaer & Tompa, 1965; Blanc *et al.*, 1991). However, this approach cannot be used in situations where there is a contribution to the transmission function that varies from point to point across the crystal in a way that is not related to the crystal morphology, as is the case for gasket shadowing or absorption by the pressure medium. The integral within the transmission function therefore has to be approximated by a summation over a set of grid points in the crystal. If a grid of equally spaced points is employed for this calculation, a very large number of points are required in order to ensure a reasonable approximation (say within 0.1%) of the integral. Therefore, *Absorb* is coded to set up a Gaussian grid of unequally spaced points over which the path length calculation is performed (cf. Busing & Levy, 1957; Wuensch & Prewitt, 1965; Burnham, 1966). The approximation for the transmission function in equation (4) becomes

$$T = V^{-1} T(\Psi_I) T(\Psi_D) \sum_{i,j,k} w_i w_j w_k \exp[-\mu_x(t_{1,x} + t_{D,x})] \times \exp[-\mu_g(t_{1,g} + t_{D,g})] \exp[-\mu_m(t_{1,m} + t_{D,m})]. \quad (8)$$

Each individual term inside the summation represents the transmission function for the incident beam to a particular point within the crystal, together with the diffracted beam from that point to the detector. The w_i , w_j , w_k are weights pre-assigned to each grid point to compensate for the unequal spacing of the points. The volume of the crystal model can be obtained as $V = \sum_{i,j,k} w_i w_j w_k$. Tests indicate that the summation in equation (8) usually converges to within 0.1% of the true value of the integral with 16 points or less along each of three axes provided that $\mu t \leq 10$. The option to use a finer 32-point grid for $\mu t \geq 10$ or a coarser grid for less-absorbing conditions is provided within *Absorb*. Further details about the absorption corrections made by this method of calculation can be found in the original paper describing the *Absorb* program (Burnham, 1966) and in the *International Tables for Crystallography* (Vol. C, §6.3.3.4).

Within *Absorb*, the calculation of the path length of a beam within the crystal is performed by the method described by Burnham (1966) and Wuensch & Prewitt (1965), which requires that each of the faces of the crystal be described in the form of an equation

$$Ax + By + Cz + D = 0, \quad (9)$$

with the coordinates x , y , z referenced to the φ -axis coordinate system. In *Absorb* these equations are derived internally from the user-supplied description of the crystal. This description can be in the

form of the coordinates of the corners in the φ -axis system, which is found to be the most useful form for crystals in the DAC. In this case the equations of all potential bounding planes are formed from all possible triplets of specified corners. The true bounding planes are identified as those for which all of the listed corners obey the condition that $Ax + By + Cz + D \leq 0$. Alternatively, the faces of the crystal can be specified in terms of their Miller indices hkl and their perpendicular distance d from the origin point of the φ -axis system. The three parameters A , B and C of the plane equation are equal to the three direction cosines of the plane normal in the φ -axis system. They are therefore obtained as the three components of the vector $\mathbf{UB} \cdot \mathbf{h} / |\mathbf{UB} \cdot \mathbf{h}|$ with $D = -d$. Once the plane equations have been derived in the form of equation (9) from the user-specified information, the path calculation for each beam to and from each grid point in the crystal is performed by the method of Wuensch & Prewitt (1965), making use of the direction cosines of the incident and diffracted beams.

In order to calculate the path lengths of a beam within the gasket and the pressure medium, it is assumed within the *Absorb* program that the anvil surfaces are parallel and coincident with the surfaces of the gasket. There is no allowance for 'bulging' of the gasket around the anvils because this should only affect beams at very high values of Ψ , which will be obscured by the other components of the DAC. Further, it is assumed that the gasket hole is a right-circular cylinder with an axis parallel to the axis of the DAC: it has the same radius at all depths through the gasket. The latter, of course, cannot be measured and calculations are forced to assume that 'gasket barreling', in which the radius of the gasket hole is greater towards the center of its thickness than at the surfaces in contact with the diamonds, does not occur.

Given these assumptions, the total path length of a beam within the diamond cell is determined from the y coordinate of the point and the direction cosine of the beam with respect to the y axis (Fig. 3), $t(\text{total}) = \Delta y / \cos \Psi$. The value of Δy is either the y coordinate of the point or $t_g - y$ (Fig. 3). The beam path to a given point in the crystal cuts the plane of the anvil culet face at a radius from the cell axis of $R(\text{beam}) = (\Delta y \tan \Psi_D + R_x)$, where $R_x = \pm(x^2 + y^2)^{1/2}$ (Fig. 3). The correct sign of R_x can be determined from the direction cosine of the beam to the x axis. Clearly, if $R(\text{beam})$ is less than the radius of the gasket hole r_g , then the beam does not intersect the gasket and that point is not shadowed. If $r_g > R(\text{beam})$, then the point is shadowed by the gasket and the path length in the gasket is $[R(\text{beam}) - r_g] / \sin \Psi$. The path length in the pressure medium is then calculated as the total path length in the cell less the path lengths in the crystal and the gasket.

When the sample crystal is formed by condensing gases or fluids *in situ* in the DAC, the crystal fills the gasket hole (e.g. Miletich *et al.*, 2000) and this allows the effect of gasket shadowing to be calculated analytically (e.g. Santoro *et al.*, 1968), especially if the crystal is non-absorbing and the gasket is considered opaque (Von Dreele & Hanson, 1984). While these filled gasket cases could be explicitly coded, the approach used within the *Absorb* program for these cases is to set up a grid of points representing the crystal that spans the entire volume of the gasket hole. The total path length within the cell and the path length in the gasket are calculated for each beam to each grid point as described above. The path length in the crystal is then simply the difference between these two values.

3.4. Code validation

As noted by many authors (including Cahen & Ibers, 1972; Alcock, 1974; Flack *et al.*, 1980) it is very difficult to validate the correct

operation of all parts of a computer code for calculating transmission functions, especially because the calculations are based upon numerical approximations to integrals. The *Absorb* code provides values for the transmission function of crystals in air that agree to within rounding error with the standard test values tabulated by Cahen & Ibers (1972) and Flack *et al.* (1980), provided that the integral is approximated by a fine-enough Gaussian grid. As an approximate guide, a grid of 8 or 16 points along each axis is sufficient up to $\mu t \simeq 10$, but 32 point grids are required for accuracy at the 0.1% level for $\mu t \simeq 100$. Alternative descriptions of the same model of faceted crystals provide values of the transmission function that agree to about 1 part in 10000, which is the expected level of uncertainty and indicates that the conversion routines within the *Absorb* program for the various types of crystal description are at least internally consistent. The transmission functions for a spherical crystal calculated with 16 grid points per axis agree to within 1 part in 1000 with those calculated analytically and listed in Table 6.3.3.3 of Maslen (1992) for μR from 0.1 to 2.5. Comparisons with other absorption codes for crystals in air have not revealed any discrepancies greater than those expected from rounding errors and limitations in the numerical methods.

Some simple limiting cases of DAC shadowing can be compared with analytic solutions. For $\Psi < 40^\circ$, the shadowing factors of a non-absorbing crystal that completely fills the gasket hole of an opaque gasket are within 0.2% of those calculated analytically (Von Dreele & Hanson, 1984), but the discrepancy increases to 1% for $\Psi > 50^\circ$,

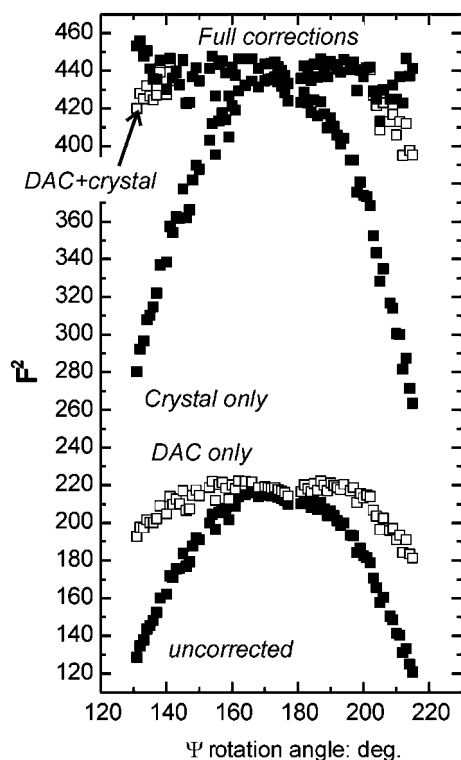


Figure 4

The variation of intensity (bottom) with Ψ rotation of the $2\bar{2}0$ reflection measured at 1.0° intervals in Ψ_{rot} from a crystal of CaSnO_3 in a DAC. Data were collected with ω scans on an Xcalibur-1 instrument equipped with a point detector. The Ψ angle of 171° corresponds to $\varphi = 0^\circ$, the position of minimum cell absorption, at which point $\Psi_1 = 11.7^\circ$ and $\Psi_D = 9.1^\circ$. The inclination angles Ψ_1 and Ψ_D both increase to $\sim 43^\circ$ at the extreme values of Ψ_{rot} shown. The data corrected for the absorption by individual cell components or the crystal show less variation than the uncorrected data, but the inclusion of the effect of gasket shadowing is required to eliminate all of the measured intensity variation (topmost filled symbols).

which is not of practical importance. The 'filled gasket' case can be closely simulated by describing the crystal as a polyhedral prism whose edges touch the edge of the gasket hole and whose length is the thickness of the gasket. Transmission factors from the prism model differ from the analytic solutions by up to 1%, as expected from the fact that the prismatic crystal does not completely fill the gasket hole. Despite the expected discrepancies of around 1%, this prism test can be performed for any of the combinations of opaque and absorbing gaskets with absorbing and non-absorbing crystals for which analytic solutions are not available.

3.5. Data input and output

The details of the experimental configuration necessary to calculate the transmission function are supplied to the *Absorb* program in an ASCII text file. Following the concept of the CIF, all of the lines in the file are labeled, allowing the data to appear in any order in this 'experiment file'. This structure also has the utility of allowing the instructions for new methods to be easily incorporated into *Absorb* itself as well as the development of related utilities such as a GUI-based editor for the absorption model that could include graphical display of the crystal model and the direct importation of video images of the crystal. It will also provide the opportunity to develop a refinement program for the crystal model itself that has been found to improve the precision of the absorption correction in some cases (*e.g.* Kuhs *et al.*, 1996).

The information required in the experiment file includes details of the configuration of the diffractometer including the radiation wavelength, the circle parities, and the axial orientation used by the diffractometer control software for the UB matrix. This allows the program to be used with data from any diffractometer without the need to recode the software (*cf.* Cahen & Ibers, 1972). The details of the crystal shape are specified in the experiment file either by the coordinates of the corners in the φ -axis system, or by the Miller indices of the bounding faces and their perpendicular distance from the origin. In the latter case, the UB matrix must be supplied as well. The absorption coefficient of the crystal can either be input as a value, or the unit-cell contents and volume can be specified, in which case the value of the absorption coefficient is calculated from the mass absorption coefficients tabulated in the 1992 edition of Vol. C of the *International Tables for Crystallography*. The details of the diamond-anvil cell are also supplied in the experiment file in one of the several ways described in the preceding text.

As noted above, *Absorb6.0* will read reflection data in the HKLF4 format used by *SHELX*, provided that beam path information is also present as the direction cosines with respect to the crystal axes. In order for these direction cosines to be used by the program, the user has also to specify the UB matrix in the experiment file. The *RFINE* int format is also accommodated, which is specifically designed for point-detector data and includes the beam path information as the diffractometer setting angles for each reflection. The absorption-corrected data can be written in either the HKLF4 format or the *RFINE* abs/avg format. The latter also contains a function of $\bar{T} = -(1/T)(\partial T/\partial \mu)$ necessary for the correct calculation of extinction corrections within the refinement program. Details of the absorption calculations are also provided in an ASCII log file and a CIF.

3.6. Examples

Fig. 4 provides a graphical example of the relative effects of the crystal and diamond-anvil cell absorption as calculated by the program *Absorb6.0*. The sample crystal is CaSnO_3 perovskite with $\mu_1 = 122.5 \text{ cm}^{-1}$ loaded in a DAC of the ETH design (Miletich *et al.*,

Table 1
Results of absorption correction for CaSnO₃ data.

R_{int} was calculated for all 73 reflections in the data set.

Corrections applied	T (range)	R_{int}
None	1.000	0.127
Crystal	0.459–0.498	0.110
DAC	0.667–0.982	0.037
Crystal + DAC	0.306–0.485	0.022
Crystal + DAC + gasket	0.274–0.485	0.014

Table 2
Instructions in the experiment file for the CaSnO₃ example.

```
CELL 5.5022 5.6508 7.8656 90.0 90.00 90.00 244.5543
WAVEL 2 0.709260 0.713543 0.500000
PARITY 1,1,1,1
BLAXES 1,2,3

CONTENTS CA1 SN1 O3 Z = 4
ABSORB MODEL XYZCORNER 5,5,5,0
ABSORB CORNER 68.0,0.0,32.0
ABSORB CORNER -49.0,0.0,61.0,
ABSORB CORNER -74.0,0.0,-32.0
ABSORB CORNER 68.0,60.0,32.0,
ABSORB CORNER -49.0,60.0,61.0,
ABSORB CORNER -74.0,60.0,-32.0
ABSORB CORNER 43.0,0.0,-60.0
ABSORB CORNER 43.0,60.0,-60.0

DAC TYPE 5,
DAC OPEN 45.,45.
DAC ABSPSI CURVE 0.55
DAC GASKET 114.0,125.,300.0,0.2
```

Table 3
Instructions in the experiment file for the YAIO₃ example.

```
UBL -.103486 -.085802 0.010385
UBL -.083083 0.100510 0.023682
UBL -.032799 0.016089 -.092681
WAVEL 2 0.709260 0.713543 0.500000
MONO 1 12.2000 90.0000 0
BLAXES -2,1,3

ABSORB MU 290.95
ABSORB MODEL XYZCORNER 4,4,4,0
ABSORB CORNER 102.3, 0.0,53.8
ABSORB CORNER -98.6, 0.0, 58.1
ABSORB CORNER -72.2, 0.0,-77.3
ABSORB CORNER 88.9, 0.0,-57.3
ABSORB CORNER 102.3,32.0, 53.8
ABSORB CORNER -98.6,32.0, 58.1
ABSORB CORNER -72.2,32.0, -77.3
ABSORB CORNER 88.9, 32.0, -57.3

DAC TYPE 5,
DAC OPEN 40.,40.
DAC GASKET 120.0,164.,300.0,0.2
DAC ABSPSI CURVE 0.347
```

2000). The diamond anvils, 1.6 mm thick, were mounted on Be platens 4 mm thick, with Be plugs filling the optical access holes. The data are all from the 220 reflection of the perovskite, collected with standard ω scans at 1° intervals in Ψ (*i.e.* rotation about the 220 plane normal) on an Xcalibur-1 diffractometer equipped with a point detector. The data were integrated and reduced to structure factors with the *WinIntegrStp* program (Angel, 2003). Twelve individual reflections were removed from the data set because their intensities were affected by simultaneous diffraction events in the diamond anvils (Loveday *et al.*, 1990) similar to those shown in Fig. 2. Normally these reflections would be included in the calculation of absorption corrections and only subsequently identified and excluded. But in this case they were removed first in order to provide a clearer illustration of the operation of the *Absorb* program.

Without any absorption corrections the data show a strong fall-off with Ψ rotation angle as the inclination angles of both the incident and diffracted beams to the DAC axis increase (Fig. 4), and the R_{int} value for these uncorrected data is very poor (Table 1). Separate corrections for the absorption by the diamond anvils and Be backing plates alone, or the crystal alone, do improve the self-consistency of the data (Table 1), but only the combination of the two provides good agreement between the reflections across the majority of the range of the Ψ scan. Close inspection of Fig. 4 shows that the F^2 values corrected for absorption by the cell components and the crystal together (labelled 'DAC + crystal') still show a significant decrease at the extremes of the scan. This is due to gasket shadowing at high inclination angles Ψ_I and Ψ_D . The addition of a correction for this effect reduces R_{int} from 0.022 to 0.014 for all of the reflections (Table 1). Table 2 provides a listing of the experiment file for the complete set of corrections for these measurements. The partial corrections were achieved by simply deleting the appropriate instructions from the experiment file. Note that the absorption by the cell components is specified by a single parameter curve, the crystal is described in terms of the Cartesian coordinates of its corners, and the indented steel gasket ($\mu_1 \approx 300 \text{ cm}^{-1}$) has a thickness of 114 μm and was drilled with a hole 125 μm in radius. The absorption by the methanol–ethanol pressure fluid was considered insignificant and was therefore not included in the calculations. Because the data set was integrated with the *WinIntegrStp* program (Angel, 2003), the data file input into *Absorb* includes the setting angles in Busing–Levy parities so the UB matrix is not required to be listed in the experiment file.

Table 3 lists an experiment file for the absorption corrections applied to the full data set collected with a Sapphire-II CCD detector on an Xcalibur-2 diffractometer from a YAIO₃ perovskite crystal loaded in a DAC. The *CRYSTALIS* integration software (Oxford Diffraction, 2003) reduces the CCD images to a data file with the *SHELXL* HKLF4 format, which includes direction cosines of the incident and diffracted beams relative to the crystallographic axes of the sample. Therefore, the experiment file also includes the UB matrix from the *CRYSTALIS* software to allow the *Absorb* program to calculate direction cosines of these beams relative to the Busing–Levy φ -axis system. Because the entries in the UB matrix have been multiplied by the wavelength the entries in the experiment file are labeled UBL. The *CRYSTALIS* UB matrix is referenced to a different choice of Cartesian axes from those of Busing & Levy (1967) and the relationship is specified by the BLAXES card. Otherwise the entries are equivalent to those for the CaSnO₃ example listed in Table 2. The application of the absorption correction reduces R_{int} for all reflections from 0.052 to 0.042, but makes no change to $R_{\text{int}} = 0.028$ for the reflections not rejected by the averaging program, which excludes outliers on the basis of the criteria of Blessing (1987). This is not an unusual situation. In this case it arises because the orthorhombic crystal was oriented with its [110] axis approximately parallel to the load axis of the DAC. Therefore, symmetry-equivalent reflections have similar values of Ψ_I and Ψ_D and thus have similar transmission functions. However, refinement of the crystal structure from the data set uncorrected for absorption yields significantly larger R values and bond lengths and angles that are shifted by more than 3 standard uncertainties from the values obtained from the absorption-corrected data set.

Further examples of the description of less-common experimental configurations for input to the *Absorb* program are provided in the manual that accompanies the distribution. Applications of earlier versions of the program are described by, for example, Allan *et al.* (1998), Miletich *et al.* (1998), Angel *et al.* (2001), Armbruster *et al.* (2001), and Friedrich *et al.* (2002).

4. Conclusions

The calculation of the transmission function of reflections from a crystal held in a transmission-geometry DAC can be achieved in either of two ways. If there is no shadowing of the crystal by the gasket or absorption by the pressure medium, then the crystal transmission function can be calculated by any absorption program and the transmission function for the DAC alone can be applied separately, as expressed by equation (3). If, on the other hand, there is either gasket shadowing or absorption by the pressure medium, then the transmission function for these components of the sample assembly varies across the crystal and a dedicated program such as *Absorb* must be used to implement equation (4). *Absorb* does, however, also function as a normal absorption program for crystal data collected in air and could be further extended to handle other DAC geometries and the absorption of other environmental devices, such as furnaces.

The *Absorb* program is available for academic use by download as a zip archive from <http://www.crystal.vt.edu/>. The program executable is accompanied by example files that illustrate the use of the program in several modes, as well as a comprehensive manual.

I wish to acknowledge Charles W. Burnham for his original coding of the *Absorb* program and Larry Finger for further developments of the code. Recent developments of this software were supported by NSF grant EAR-0105864 to N. L. Ross and RJA. Many users have undertaken testing of the program and provided significant feedback, especially David Allan, Simon Parsons and their colleagues at the University of Edinburgh, and Jason Burt, Ronald Miletich, Tiziana Boffa-Ballaran, Demelza Hugh-Jones, Jing Zhao and Nancy Ross.

References

- Ahsbahs, H. (1987). *Prog. Crystal Growth Charact.* **14**, 263–302.
- Alcock, N. W. (1974). *Acta Cryst.* **A30**, 332–335.
- Allan, D. R., Clark, S. J., Parsons, S. & Ruf, M. (2000). *J. Phys. C Condens. Mater.* **12**, L613–L618.
- Allan, D. R., Kelsey, A. A., Clark, S. J., Angel, R. J. & Ackland, G. J. (1998). *Phys. Rev. B*, **57**, 5106–5110.
- Allan, D. R., Miletich, R. & Angel, R. J. (1996). *Rev. Sci. Instrum.* **67**, 840–842.
- Angel, R. J. (2003). *J. Appl. Cryst.* **36**, 295–300.
- Angel, R. J., Downs, R. T. & Finger, L. W. (2000). *High-Pressure and High-Temperature Crystal Chemistry*, edited by R. M. Hazen & R. T. Downs, pp. 559–596. Washington, DC: Mineralogical Society of America.
- Angel, R. J., Mosenfelder, J. L. & Shaw, C. S. J. (2001). *Phys. Earth Planet. Int.* **124**, 71–79.
- Armbruster, T., Kohler, T., Libowitzky, E., Friedrich, A., Miletich, R., Kunz, M., Medenbach, O. & Gutzmer, J. (2001). *Am. Mineral.* **86**, 147–158.
- Arndt, U. W. & Willis, B. T. M. (1966). *Single Crystal Diffractometry*. Cambridge University Press.
- Blanc, E., Schwarzenbach, D. & Flack, H. D. (1991). *J. Appl. Cryst.* **24**, 1035–1041.
- Blessing, (1987). *Crystallogr. Rev.* **1**, 3–58.
- Boldyreva, E. V., Naumov, D. Y. & Ahsbahs, H. (1998). *Acta Cryst.* **B54**, 798–808.
- Burnham, C. W. (1966). *Am. Mineral.* **51**, 159–167.
- Busing, W. R. & Levy, H. A. (1967). *Acta Cryst.* **22**, 457–464.
- Busing, W. R. & Levy, H. A. (1957). *Acta Cryst.* **10**, 180–182.
- Cahen, D. & Ibers, J. A. (1972). *J. Appl. Cryst.* **5**, 298–299.
- D'Amour, H., Schiferl, D., Denner, W., Schulz, H. & Holzapfel, W. B. (1978). *J. Appl. Phys.* **49**, 4411–4417.
- Dera, P. & Katrusiak, A. (1998). *Acta Cryst.* **A54**, 653–660.
- DeTitta, G. T. (1985). *J. Appl. Cryst.* **18**, 75–79.
- Finger, L. & Prince, E. (1974). *A System of Fortran-IV Computer Programs for Crystal Structure Computations*. National Bureau of Standards Technical Note 854. Washington, DC: NBS.
- Finger, L. W. & King, H. (1978). *Am. Mineral.* **63**, 337–342.
- Flack, H. D., Vincent, M. G. & Alcock, N. W. (1980). *Acta Cryst.* **A36**, 682–686.
- Friedrich, A., Lager, G. A., Ulmer, P., Kunz, M. & Marshall, W. G. (2002). *Am. Mineral.* **87**, 931–939.
- Hazen, R. M. (1976). *Am. Mineral.*, **61**, 266–271.
- Kuhs, W. F., Bauer, F. C., Hausmann, R., Ahsbahs, H., Dorwarth, R. & Holzer, K. (1996). *High Press. Res.* **14**, 341–352.
- Loveday, J. S., McMahon, M. I. & Nelmes, R. J. (1990). *J. Appl. Cryst.* **23**, 392–396.
- Malinowski, M. (1987). *J. Appl. Cryst.* **20**, 379–382.
- Maslen, E. (1992). *International Tables for X-ray Crystallography*, Vol. C, edited by A. Wilson, pp. 520–529. Dordrecht: Kluwer Academic Publishers.
- Meulenaer, J. de & Tompa, H. (1965). *Acta Cryst.* **19**, 1014–1018.
- Miletich, R., Allan, D. R. & Kuhs, W. F. (2000). *High-Pressure and High-Temperature Crystal Chemistry*, edited by R. M. Hazen & R. T. Downs, pp. 445–519. Washington, DC: Mineralogical Society of America.
- Miletich, R., Seifert, F. & Angel, R. J. (1998). *Zeit. Kristallogr.* **213**, 288–295.
- Oxford Diffraction (2003). Wrocław, Poland.
- Santoro, A., Weir, C. E., Block, S. & Piermarini, G. J. (1968). *J. Appl. Cryst.* **1**, 101–107.
- Scheidegger, S., Estermann, M. & Steurer, W. (2000). *J. Appl. Cryst.* **33**, 35–48.
- Von Dreele, R. B. & Hanson, R. C. (1984). *Acta Cryst.* **C40**, 1635–1638.
- Wittlinger, J., Werner, S. & Schulz, H. (1997). *Phys. Chem. Miner.* **24**, 597–600.
- Wunsch, B. J. & Prewitt, C. T. (1965). *Zeit. Kristallogr.* **122**, 24–59.